Applied Water Science (2023) 13:63
https://doi.org/10.1007/s13201-023-01867-9

ORIGINAL ARTICLE

Biosorption of metronidazole using *Spirulina platensis* microalgae: process modeling, kinetic, thermodynamic, and isotherm studies

Zahra Esmaili[1] · Behnam Barikbin[1] · Mahmoud Shams[1,2] · Hossein Alidadi[1,2] · Tariq J. Al-Musawi[3] · Ziaeddin Bonyadi[1,2]

Received: 24 August 2022 / Accepted: 3 January 2023 / Published online: 12 January 2023

Abstract

Metronidazole is well-known antibiotic which, globally, ranks high in popular usage. Therefore, traces of residues of this antibiotic were identified in aquatic bodies. A photosynthetic cyanobacterium, of the microalgae category, *S. platensis*, has been found to be efficient in the removal of this antibiotic. This study was performed to evaluate the efficiency of *S. platensis* in the removal of metronidazole from aqueous environments. To set up the optimum conditions for facilitating metronidazole removal, BBD model was employed. The experiment included the following parameters: the initial metronidazole level (10–80 mg/L), pH (4–10), contact time (10–60 min), and biomass dose (0.1–0.5 g/L). From the findings it was evident that *S. platensis* was able to remove 88.15% of the metronidazole under the following conditions: contact time 38.05 min, metronidazole level 35 mg/L, pH 7.71 and a biomass dose 0.3 g/L. The quadratic model revealed that metronidazole concentration was the chief variable that influenced its removal rate. MNZ removal rate was observed to follow the pseudo-second-order model and the Freundlich model. From the thermodynamic data it appeared that the process of metronidazole biosorption was spontaneous, exothermic and physical. The results of this study revealed that *S. platensis* could be used as an inexpensive and efficient biosorbent to remove the metronidazole from aqueous solutions.

Keywords Antibiotic · Metronidazole · *Spirulina platensis* · Biosorption · Box–Behnken model

✉ Tariq J. Al-Musawi
tariq.jwad@mustaqbal-college.edu.iq

✉ Ziaeddin Bonyadi
Bonyadiz@mums.ac.ir

Zahra Esmaili
Esmailiz2@mums.ac.ir

Behnam Barikbin
Barikbinb@mums.ac.ir

Mahmoud Shams
Shamsmh@mums.ac.ir

Hossein Alidadi
Alidadih@mums.ac.ir

[1] Social Determinants of Health Research Center, Mashhad University of Medical Sciences, Mashhad, Iran

[2] Department of Environmental Health Engineering, School of Health, Mashhad University of Medical Sciences, Mashhad, Iran

[3] Building and Construction Techniques Engineering Department, Al-Mustaqbal University College, Hillah, Babylon 51001, Iraq

Abbreviations

S. platensis	*Spirulina platensis*
BBD	Box–Behnken design
MNZ	Metronidazole
FT-IR	Fourier-transform infrared spectroscopy
SEM	Scanning electron microscopy
BET	Brunauer–Emmett–Teller
RSM	Response Surface Methodology
pHzpc	Zero point of charge
ANOVA	Analysis of variance

Introduction

Slowly becoming prominent as contaminants entering into aquatic bodies via the municipal and industrial wastewater are a variety of compounds (Gondi et al. 2022). These include pesticides, disinfectant byproducts, and antibiotics (Pirsaheb et al. 2013; Gilca et al. 2020). Antibiotics used in the treatment of some bacterial infections form a big pollutant class (Polianciuc et al. 2020). Most of them are resistant to biological treatments

and their concentration has been observed to show a gradual rise in both water and soil (Bonyadi et al. 2021).

MNZ, an antibiotic of the nitroimidazole family, is commonly used in the treatment of bacterial infections as it helps to decrease inflammation. It finds use in the treatment of parasitic diseases in poultry and fish as well (Malakootian et al. 2019). Despite its efficacy in the treatment of various diseases, the use of MNZ is often linked to problems related to health and the environment. MNZ is circular in structure and causes damage to the DNA of the lymphocytes. This pollutant has the potential to be carcinogenic and mutagenic in humans (Farzadkia et al. 2015). The two significant properties of this contaminant are its low degradability and high solubility in aqueous solutions. It is these characteristics that lower the efficiency of its removal through the use of a variety of purification methods. Therefore, it is crucial to remove the MNZ from aquatic environments employing effective techniques (Jiang et al. 2018). From a variety of studies, it is obvious that several methods like chlorination chlorination (Wang et al. 2020), adsorption (Tang et al. 2021), use of nanoparticles (Adel et al. 2021), and oxidation (Brito et al. 2021) are being employed for antibiotic removal from aqueous solutions. Despite the efficacy of these techniques in MNZ removal, these are frequently related to some disadvantages, namely, high cost of investment and operation, large production of sludge and byproducts (Adel et al. 2021). Only in recent times has the application of biological processes in environmental pollutant removal garnered favorable attention, as these have been found environmentally friendly, involve low cost of investment, have good efficacy in pollutant removal and produce lower volume of sludge (Sadeghi et al. 2019).

In some recent studies, different algae have been used as special biosorbents to treat a variety of wastewaters and polluted waters (Jayakumar et al. 2021; Kiki et al. 2021). With their high adsorption capacity caused by the carboxyl, sulfonate, hydroxyl and amine groups present on their surfaces, these algae show promise (Nasoudari et al. 2021). *S. platensis,* a photosynthetic cyanobacterium, belongs to the microalgae group. These occur most frequently in saline waters, like seas and lakes (Liliana et al. 2021).

The aim of this paper is the elimination of metronidazole from the aqueous medium using *S. platensis* (as a biosorbent). The MNZ removal process was also explored to attain a clearer understanding of the biosorption mechanism employing isotherm, kinetic, and thermodynamic studies.

Materials and methods

Chemicals and reagents

The Sigma-Aldrich Company (Germany) was the suppliers of the MNZ antibiotic. The synthetic solutions prepared at different concentrations were done using the MNZ stock solution of 500 mg/l through dilution with deionized water. Merck (Germany) supplied the other chemicals also used in this work.

Table 1 Range and levels of independent factors used for the MNZ biosorption

Factor	Code	Factor level		
		−1	0	+1
MNZ concentration (mg/L)	A	10	45	80
S. platensis dose (g/L)	B	0.1	0.3	0.5
Contact time (min)	C	10	35	60
pH	D	4	7	10

Biosorbent preparation

The organism of *S. platensis* (abdf 2224) was received from the Iranian National Algae Culture Collection, Tehran, Iran. Using Zarrouk's medium this microorganism was grown under constant light (3000 lx) and room temperature (25–27 °C). The separation of the algal cells from the medium was done using a centrifuge at 8000 rpm for 12 min. Then, the algae thus collected were dried at 60 °C for 24 h. Finally, the dried algae were placed under a dryer at room temperature and used in the biosorption experiments that followed.

Biosorbent characteristics

Employing the FTIR, SEM, and BET techniques, the biosorbent surface was investigated and characterized. The functional groups present on the *S. platensis* surface and the interaction between them and the MNZ, post the biosorption process, was measured using the FT-IR spectrometer (Broker victor 22). The *S. platensis* surface morphology was studied by applying the SEM test (MIRA3-FEG, TESCAN, Czech). Using the BET method (ASAP 2020, Micromeritics Co.) the specific surface area of the *S. platensis* was measured via the nitrogen single-layer adsorption and computed as a function of the relative pressure.

Design of experiments

As shown in Table 1, all the various variables, such as the initial MNZ level (10–80 mg/L), pH (4–10), contact time (10–60 min), and *S. platensis* dose (0.1–0.5 g/L) were examined in this study. All the experiments were performed in 250 mL flux which contained 100 mL of the synthetic mixture. A magnetic shaker (Parsazazma model, Iran) was used to agitate the synthetic solutions at 300 rpm, fixed velocity.

When the reaction time ended, sampling was done by taking 10 mL of the synthetic solution in a reaction vessel, and centrifuging it at 4000 rpm for 15 min. It was then filtered using Whatman 42 filter paper. Finally, the value of the remaining MNZ in the supernatant was assessed using the spectrophotometer at λmax of 320 nm. The following equation was applied to calculate the removal rate of MNZ:

$$\text{Removal efficiency } \% = \frac{(C_0 - Ce) \times 100}{C_0} \quad (1)$$

where C_0 is the initial MNZ concentration (mg/l), *Ce* represents the MNZ concentration in the treated solution post a given biosorption time (mg/L).

$$q_e = \frac{(C_0 - C_e)}{m} \times V \quad (2)$$

where m is the mass of the algae biosorbent (g), and *V* indicates the reaction solution volume (L).

Modeling MNZ removal

The present study employed the RSM and BBD design, to optimize the efficiency of metronidazole removal by *S. platensis*. The following equation expresses the quadratic model used by the RSM:

$$Y = \beta_0 + \sum_{i=1}^{k} \beta_i x_i + \sum_{i=1}^{k} \beta_{ii} x_i^2 + \sum_{1 \le i \le j}^{k} \beta_{ij} x_i x_j \quad (3)$$

where Y, β_0, β_i, β_{ii}, β_{ij} and x_i or x_j represent the predicted response, constant coefficient, regression coefficients for linear impacts, quadratic coefficients, interaction coefficients, and the coded values of the factors, respectively.

Isotherm, kinetic and thermodynamic studies

For selection of the best isotherm model from the Freundlich, Langmuir and Tamkin isotherms, a series of experiments was conducted under conditions which included MNZ concentration of 10 to 150 mg/L, pH of 7.7 and algae dose of 0.3 g/L.

The kinetic studies performed also constitute a crucial part of the sorption check which gives significant information to design a large-scale treatment system. Therefore, maintaining the same variables cited above, the kinetic studies were done fitted to pseudo-first-order, pseudo-second-order, and intra-particle diffusion models.

In the thermodynamic experiments, testing of the samples was performed at different temperatures (from 15 to 45 °C) keeping the other parameters fixed as listed: MNZ concentration of 35 mg/L, pH of 7.7, *S. platensis* dose of 0.03 g/L, and contact time of 35 min.

Regeneration study

Economically speaking, adsorbent reuse is very significant in the removal of contaminants from aquatic bodies. In this study, the initial step was to select the suitable condition (acidic or alkaline) as the adsorbent was influenced by both acidic (pH = 4) and alkaline (pH = 10) solutions. After a series of adsorption and desorption tests was done, the efficiency of the adsorbent was found to be greater under alkaline conditions. Hence, the biosorbent regeneration process was performed in an alkaline solution. The experiments were then conducted by maintaining the optimized parameters and regenerated sorbent.

Results

Characterization analysis

Using the FTIR method, analysis was done of the functional groups present on the biosorbent and their effects on MNZ removal. In Fig. 1 the FTIR spectra of fresh and used *S. platensis* are shown. Prior to the removal of the MNZ, the FTIR spectrum of the biosorbent showed the different main intense bands, around 3300, 2961, 2924, 2851, 1657, 1540, 1454, 1398, 1239, 1151, 1079, 697, 668, and 623 cm^{-1} (Fig. 1A). The peak observed at 3300 cm^{-1} was correlated to the O–H bond stretching, overlapping with the NH_2 group. The adsorption peaks noted at 2961, 2924, and 2851 cm^{-1} were caused most likely by the stretching vibrations of the CH3 and CH2 groups. In Fig. 1B, the situation of a few of the peaks revealed changes post the MNZ biosorption. The change of the 33,300 cm^{-1} peak

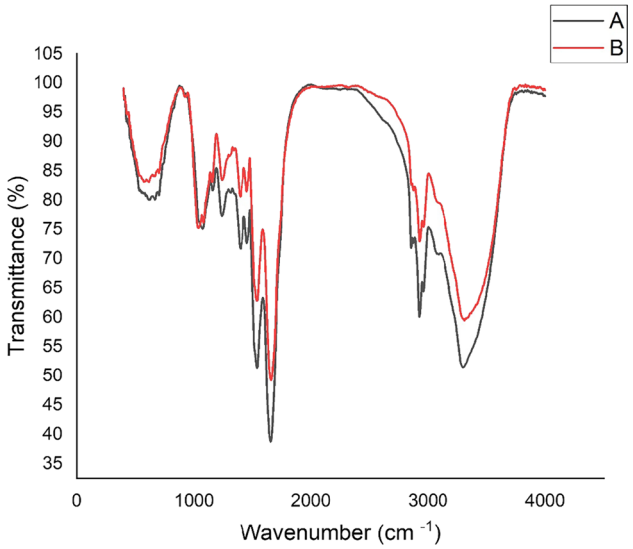

Fig. 1 FTIR Spectra of (**A**) before and (**B**) after MNZ biosorption

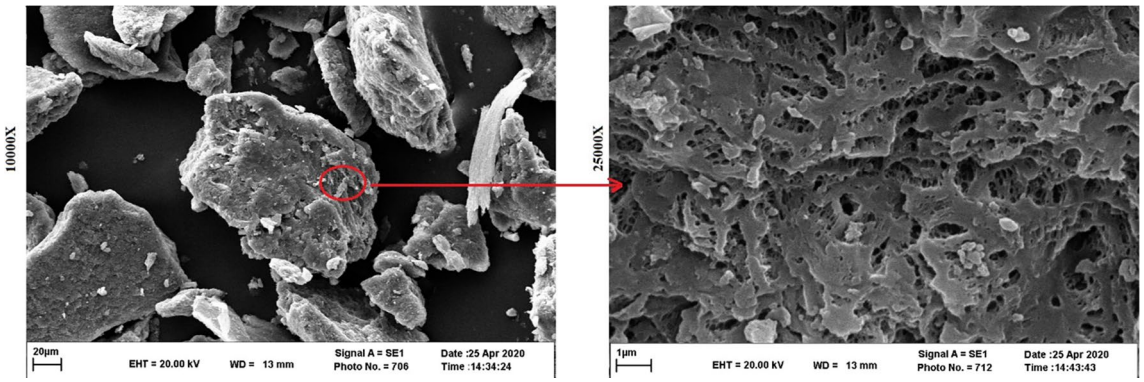

Fig. 2 SEM Images of *S. Platensis*

Table 2 Surface and pore characteristics of *S. platensis*

Mean pore diameter (nm)	Total pore volume (cm^3/g)	Surface (m^2/g)
0.24	0.0011	18.02

to 3313 cm^{-1} enables the MNZ to get attached onto the –OH and –NH groups (Kousha et al. 2013). The change in the peak at 1657.38–1660.39 cm^{-1} indicates that the C=O group is involved. Furthermore, the peak at 1073.94 cm^{-1} is altered to 1039.19 cm^{-1}, revealing that a carboxylate group (COO–) is involved in the adsorption of MNZ molecules (Nath et al. 2015).

Figure 2 reveals the raw SEM of *S. platensis*. From the SEM analysis the *S. platensis* surface is observed to be irregular and with the presence of various pores. The effective adsorption of the MNZ molecules occurs in these pores. Thus, it can be deduced that this alga possesses an extensive and accessible surface for the biosorption of the MNZ.

From the BET analysis shown in Table 2, the *S. platensis* clearly shows a specific surface area of 0.2477 m^2/g. Further, the average diameter and total volume of the biomass pores were 18.026 nm (mesopore) and 0.0011 cm^3/g, respectively. The results of this study concurred with the research done by Bazzazzadeh et al (2020) (Bazzazzadeh et al. 2020).

Figure 3 indicates the influence exerted by pH on the zeta potential of *S. platensis*. This Figure shows that in this study the pHzpc for the biomass was 6.75. This signifies that the biosorbent surface carries a negative charge or a positive charge when the pH values are above or below 6.75, respectively. The pHzpc factor is one of the vital tests for the identification of the mechanisms of biosorption (Dotto et al. 2012).

Modeling of the MNZ removal efficiency

In this work, an examination was done on the ways the main variables, such as the initial MNZ concentration, *S. platensis* dose, contact time, and pH, affected the rate of MNZ removal. In Table 3 a summary is given of the effects

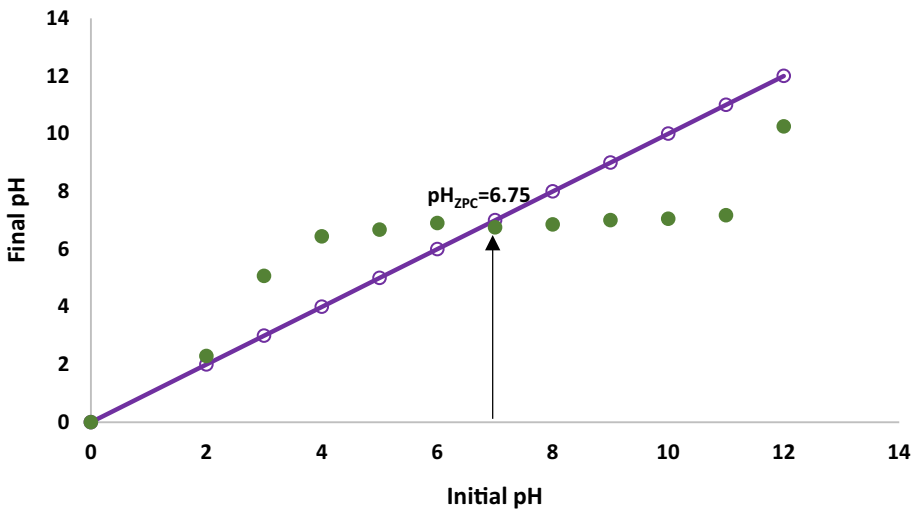

Fig. 3 Effect of pH on zeta potential of the *S. platensis*

of the four parameters that coded, as shown in Table 1, on the removal efficiency of the MNZ. The highest and lowest removal efficiencies were observed to be 88.15 and 41.41, respectively.

Design-Expert® Software approved the normality of experimental findings, a mandatory requirement for ANOVA. These findings were statistically assessed for the linear, 2Fl, quadratic and cubic models to enable the selection of the model that best explains the data. From this perspective, Table 4 provides the comparative model regression findings. Thus, for the experimental data in this study, the quadratic model was proposed as the one with the best fit.

From the results shown in Table 5, the quadratic model is revealed in Eq. 4 in terms of the coded factors of the MNZ removal rate (Y).

$$\begin{aligned} Y = {} & 85.98 - 7.52A + 3.08B + 2.92C + 3.64D \\ & + 5.26AB - 4.34AC - 5.32AD - 2.48BC \\ & - 6.57BD - 0.4CD - 15.63A^2 - 10.22B^2 \\ & - 17.14C^2 - 11.27D^2 \end{aligned} \quad (4)$$

From Eq. (4), it is obvious that each model contains both fixed and variable parts. Although the removal efficiency was 85.98%, various parameters were seen to affect it. The coded factors of A, B, C, D had the respective coefficients of -7.52, + 3.08, + 2.92, and + 3.64. The variable of A (MNZ concentration) having a coefficient value of -7.52 was the one which exerted the most effect on the removal rate. The highest interaction effect was evident in the BD, having a coefficient of value -6.57, while the highest square effects of the factors were seen in C2, which had a coefficient value of − 17.14. Conduction of similar experiments at specified optimum conditions reveals the high repeat ability of method for prediction of real removal percentage with relative deviation less than 2%.

In Table 6 ANOVA is shown for the response surface quadratic model. Normally, when the *P* value is < 0.05 it implies the significance of the model. Therefore, the R2, adjusted R2, predicted R2, and adequacy precision showed values of 0.94, 0.89, 0.70, and 12.98, respectively. For the expression of each model in Table 6, a *P* value of below 0.05 shows that the MNZ biosorption is statistically significant. The difference between the adjusted R2 and predicted R2 was suggested to be less than 0.2, which is true for this model. The signal-to-noise ratio adequacy is assessed by the precision term (Aliasghar Navaei et al. 2019). This factor showed a value of 12.98 which exceeds 4, the minimum desirable value. The adequacy of the model to predict a good outcome for the removal of MNZ

Table 3 BBD matrix for MNZ removal by *S. platensis*

Run No	Code of variable				Removal (%)	Run No	Code of variable				Removal (%)
	A	B	C	D			A	B	C	D	
1	− 1	0	0	− 1	60.04	16	1	0	0	− 1	55.58
2	0	− 1	0	1	72.53	17	0	0	0	0	82.31
3	0	0	− 1	1	62.17	18	1	1	0	0	67.58
4	0	− 1	0	− 1	52.29	19	− 1	− 1	0	0	67.26
5	− 1	1	0	0	70.08	20	0	1	1	0	62.24
6	0	0	1	− 1	57.86	21	0	0	0	0	88.15
7	1	0	0	1	49.33	22	1	0	− 1	0	42.11
8	0	1	0	− 1	63.69	23	0	0	− 1	− 1	51.00
9	0	0	0	0	86.76	24	1	− 1	0	0	43.72
10	0	0	1	1	67.42	25	0	− 1	1	0	60.32
11	− 1	0	0	1	75.06	26	− 1	0	− 1	0	50.44
12	0	1	− 1	0	63.71	27	0	0	0	0	86.76
13	0	1	0	1	57.65	28	− 1	0	1	0	67.09
14	0	0	0	0	85.93	29	0	− 1	− 1	0	51.89
15	1	0	1	0	41.41						

Table 4 Statistical adequacy evaluation of models

Source	Sequential *P* value	Lack of Fit *P* value	Adjusted R^2	Predicted R^2
Linear	0.2208	0.0012	0.0724	− 0.0019
2FI	0.8595	0.0008	− 0.0866	− 0.2093
Quadratic	< 0.0001	0.0599	0.8913	0.7028
Cubic	0.5813	0.0226	0.883	− 2.0727

Table 5 Coefficients estimation for quadratic model of MNZ removal by *S. platensis*

Factor	Coefficient Estimate	df	Standard error	95% CI low	95% CI high	VIF
Intercept	85.98	1	2	81.7	90.27	
A- Conc	−7.52	1	1.29	−10.29	−4.75	1
B- Dose	3.08	1	1.29	0.3124	5.84	1
C- Time	2.92	1	1.29	0.152	5.68	1
D- pH	3.64	1	1.29	0.8754	6.41	1
AB	5.26	1	2.23	0.4676	10.05	1
AC	−4.34	1	2.23	−9.13	0.4539	1
AD	−5.32	1	2.23	−10.11	−0.5261	1
BC	−2.47	1	2.23	−7.27	2.32	1
BD	−6.57	1	2.23	−11.36	−1.78	1
CD	−0.4025	1	2.23	−5.19	4.39	1
A^2	−15.63	1	1.75	−19.39	−11.87	1.08
B^2	−10.22	1	1.75	−13.99	−6.46	1.08
C^2	−17.14	1	1.75	−20.9	−13.37	1.08
D^2	−11.27	1	1.75	−15.03	−7.5	1.08

Table 6 Analysis of variance (ANOVA) for quadratic model of MNZ removal by *S. platensis*

Source	Sum of squares	df	Mean square	*F* value	*P* value
Model	4863.75	14	347.41	17.4	< 0.0001
A- Time	678.66	1	678.66	34	< 0.0001
B- Conc	113.74	1	113.74	5.7	0.0316
C- pH	102.2	1	102.2	5.12	0.0401
D- Dose	159.14	1	159.14	7.97	0.0135
AB	110.63	1	110.63	5.54	0.0337
AC	75.26	1	75.26	3.77	0.0726
AD	113.1	1	113.1	5.67	0.0321
BC	24.5	1	24.5	1.23	0.2866
BD	172.66	1	172.66	8.65	0.0107
CD	0.648	1	0.648	0.0325	0.8596
A^2	1584.85	1	1584.85	79.39	< 0.0001
B^2	677.98	1	677.98	33.96	< 0.0001
C^2	1904.84	1	1904.84	95.42	< 0.0001
D^2	823.37	1	823.37	41.25	< 0.0001
Residual	279.47069	14	19.96		
Lack of fit	260.07361	10	26.00	5.36	0.05
Pure error	19.39708	4	4.84		
Cor total	5143.22	28			
R^2	0.94		Predicted R^2	0.70	
Adjusted R^2	0.89		Adeq Precision	12.98	

is clearly shown in Fig. 4, where the actual removal versus the predicted removal is clearly evident.

Applying Eq. (4), the optimization study was conducted to maximize the removal of MNZ. The main parameters were in the range of the coded values of ± 1, similar to the application in the BBD. The quadratic model indicated that the maximum MNZ removal (theoretically 100%) was noted when the pH was 7.71, reaction time was 38.05 min, *S. platensis* dose was 0.3 g/L, and the MNZ concentration was 35 mg/L. Table 7 indicates the kinetic and isotherm parameters fitted for MNZ removal by *S. platensis*. The thermodynamic factors for the adsorption of MNZ onto *S. platensis* are listed in Table 8.

Discussion

Effects study

In Fig. 5a, b, the impact of the MNZ concentration, pH, contact time, and *S. platensis* dose on the MNZ removal rate is observed. From Fig. 5a, it is clear that as the MNZ concentration escalated from 10 to 80 mg/L, the removal rate correspondingly dropped by 19% (P value < 0.05). In general, in the initial step, as the MNZ concentration increased, the removal rate also showed a sharp rise seen as a steep slope, caused by the active and accessible sits present on the biomass surface; later, the curve slope is balanced because of the saturation of empty (Ramavandi et al. 2019; Zambrano et al. 2021). One of the significant factors which affects the biosorption process when this alga is used, is pH. It can change the removal efficiency by altering the biosorbent in terms of the surface charge, and the MNZ molecules in terms of the biosorbent ionization status. In Fig. 5a, a direct relationship between the MNZ concentration and biomass (P value < 0.05) is evident. Being a weak base, MNZ has a pKa1 value of 2.38 and pKa2 of 14.48, which show changes in different ways when there are alterations in the pH. When the pH drops below 4, the pollutant forms a

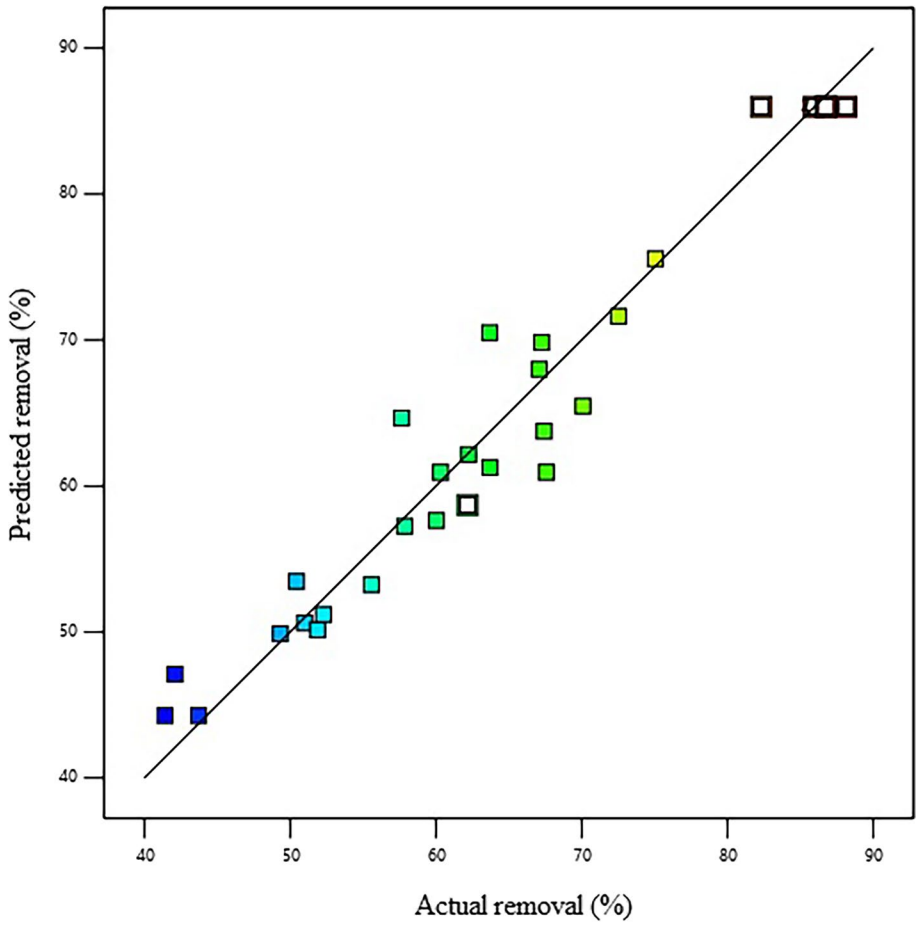

Fig. 4 Distribution of experimental versus predicted removal for MNZ biosorption onto *S. platensis*

Table 7 The kinetic and isotherm parameters fitted for MNZ removal by *S. platensis*

Kinetic Model	Linear form	Parameter	Value at different concentrations			
			10 (mg L^{-1})	50 (mg L^{-1})	100 (mg L^{-1})	150 (mg L^{-1})
Pseudo-first order	$\left(\log\left(q_e - q_t\right) = \log q_e - \frac{k_1}{2.303} \cdot t\right)$	$q_{e,\mathrm{cal}}$ [mg/g]	32.1	9.49	162.5	135.6
		K_1 [min^{-1}]	−0.002	−0.003	0.0004	−0. 002
	$\left(\log\left(q_e - q_t\right) = \log q_e - \frac{k_1}{2.303} \cdot t\right)$	R^2	0.69	0.29	0.90	0.89
Pseudo-second order	$\frac{t}{q_t} = \frac{1}{k_2 q^2} + \frac{1}{q} \cdot t$	$q_{e,\mathrm{cal}}$ [mg/g]	24.2	39.2	256	394
		k_2[min^{-1}]	0.007	0.002	0.0004	0.0003
		R^2	0.99	0.99	0.99	0.99
Intra-particle diffusion	$qt = k_p \cdot t^{0.5} + c$	k_p[mg/g $\mathrm{min}^{-0.5}$]	1.09	4.90	16.75	3.67
		R^2	0.53	0.70	0.98	0.85

Isotherm model	Linear form	Parameter	Value
Langmuir	$\frac{Ce}{qe} = \frac{Ce}{qm} + \frac{1}{qm \cdot K_L}$	qm(mg/g)	20
		K_L (L/mg)	0.20
		R^2	0.92
Freundlich	$\mathrm{Log}\, q_e = \log K_F + \frac{1}{n} \log C_e$	K_F(mg/g(L/mg)$^{1/n}$)	0.10
		n	0.71
		R^2	0.97
Temkin	$q_e = B_1 \ln \cdot k_t + B_1 \ln C_e$	k_t (L/mg)	8.96
		B_1	12.19
		R^2	0.84

Table 8 Thermodynamics parameters for MNZ sorption onto *S. platensis*

T (K)	ΔG° (kJ mol^{-1})	ΔH° (kJ/mol)	ΔS° (J $(mol\ K)^{-1}$)
288	− 17.98	− 12.63	19.59
298	− 17.58		
308	− 17.10		
318	− 16.49		

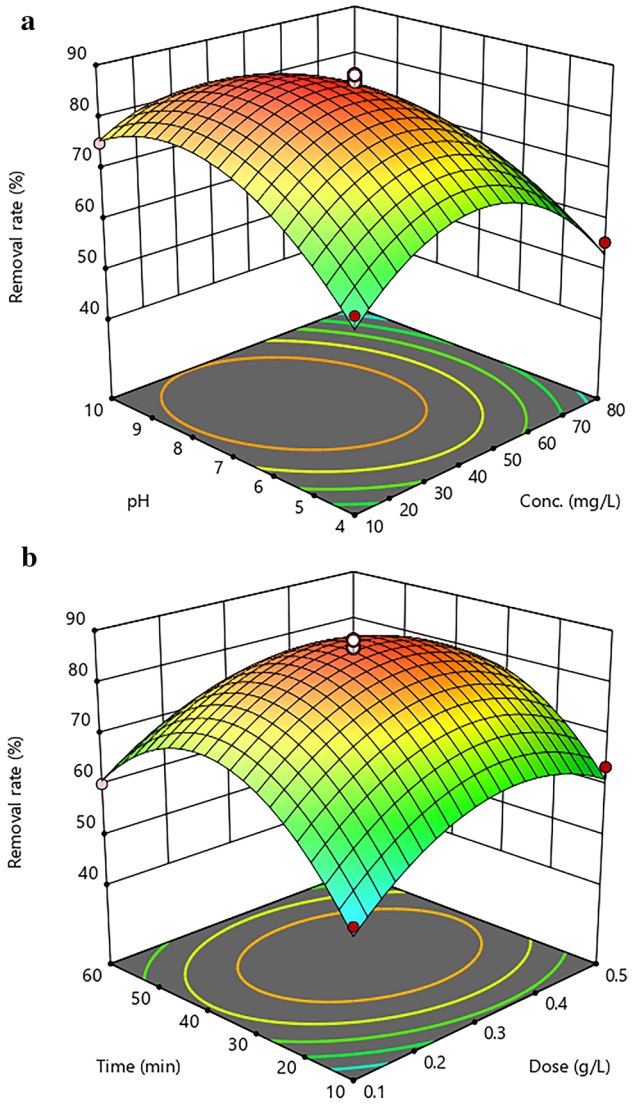

Fig. 5 Response surface plot about the effects of **a** pH versus MNZ and **b** *S. platensis* versus time

proton (MNZ-H+) as imidazoline nitrogen carries a positive charge. When pH exceeds 12, the hydroxyl groups present in the MNZ structure ionize, thus altering the charge of the MNZ to negative (MNZ-) (Nasseh et al. 2019). Further, this antibiotic carries a neutral charge when pH is in the range of 4 to 12. When the pH exceeds 6.75, the negative charge on the surface of the biomass and MNZ molecules result in lowering the removal rate again because of the repulsive electrostatic interactions. Therefore, maximum MNZ removal was anticipated when the pH value was neutral or close to the value of the zero charge of the adsorbent. Therefore, the maximum MNZ removal was expected when pH was around neutral or approaching the point of zero charge of the adsorbent (Bonyadi et al. 2021). Focusing on Fig. 5b, the inference that is drawn is that as the contact time escalates up to 38 min, the removal efficiency rises rapidly and then drops slightly (P value < 0.05). This occurs because, in the initial step, there are a large number of hollow adsorption sites, which drives the high rate of MNZ removal (Mazloomi et al. 2021).

From Fig. 5b, the efficiency of MNZ removal has a direct relationship to the rise in the *S. platensis* dose (P value < 0.05). As can be understood from Fig. 5b, when the *S. platensis* dose is raised from 0.1 to 0.3%, the removal efficiency of MNZ also correspondingly rises from 72 to 85% and then shows a slight drop. For most sorption processes this is normal behavior. Therefore, according to the biosorption theory, the pollutants are attracted onto the sorption sites present on the biosorbent surface (Kousha et al. 2013).

Adsorption kinetics

Among the most significant factors in the adsorption process is the kinetic model, which is capable of simulating the adsorption rate of the solutes from the solution-solution interface. This model, controls the velocity constants and thereby the contact time and volume of an adsorption unit, giving crucial data on the adsorption economy (Bonyadi et al. 2022). The coefficients of the reaction rate were also ascertained by applying the pseudo-first-order, pseudo-second-order and intraparticle diffusion kinetic models. From Table 7, the factors of the kinetic and isotherm fitted for the rate of removal of MNZ employing *S. platensis* are evident. In Table 7, the values of R2 for the pseudo-first-order, pseudo-second-order and intraparticle diffusion kinetics were 0.89, 0.99, and 0.85, respectively, indicating that the pseudo-second-order kinetic model was the best fit. In fact, a similar study was done by Karim et al. (2020) on MNZ adsorption onto carbon materials (Kariim et al. 2020).

Adsorption isotherms

The findings of the present study from the experimental equilibrium were evaluated using the adsorption isotherm models including the Langmuir, Freundlich and Tamkin ones. From Table 7 it is clear that the Freundlich model concurs with the equilibrium data (Wan et al. 2016). The high determination coefficient observed for the Freundlich

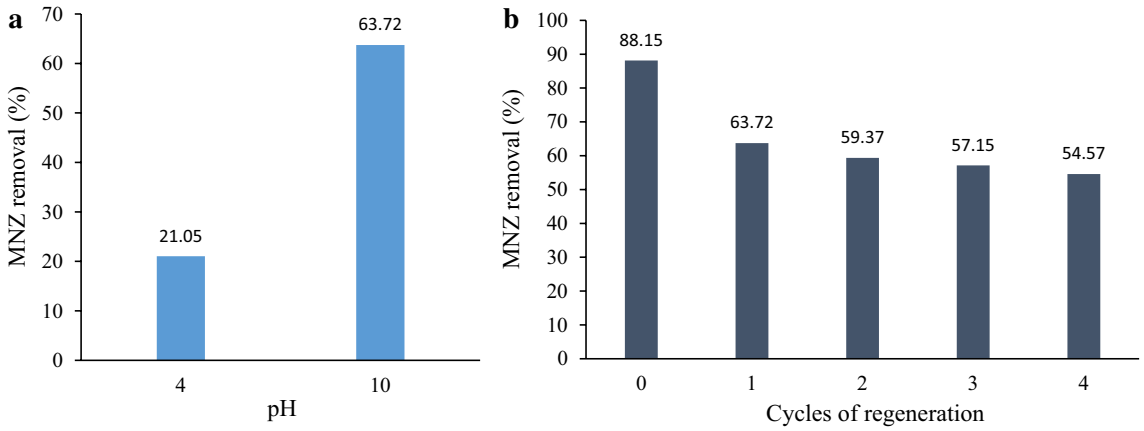

Fig. 6 Biomass reusability; MNZ removal efficiency for biomass regenerated by alkaline/acid eluting solution **a** and MNZ removal in consecutive adsorption/desorption cycles **b**

model is indicative that the MNZ adsorption onto the biomass is multilayer and heterogeneous. The Langmuir model shows that *S. platensis* has 20 mg/g as its maximum adsorption capacity.

Adsorption thermodynamic

The thermodynamic factors for the adsorption of MNZ onto *S. platensis* are listed in Table 8. These parameters indicate the possibility that the biosorption process can occur at a variety of temperatures (Danish et al. 2018). For each material the adsorption capacity may rise or fall in response to the escalating temperature, based on the type of the reaction or other factors. In fact, Table 8 shows that the negative value of ΔH° suggests that this is an exothermic process. Hence, the efficiency of the MNZ removal rises as the contact temperature decreases. In this process, the positive ΔS° value implies a rise in the irregularity of the biosorption. The negative ΔG° value suggests the characteristic of the spontaneous biosorption process. In terms of the ΔH° value (− 12.63 kJ/mol) taken from Table 8, the biosorption mechanism is principally physical (Ahmad et al. 2014).

Reusability of the *S. platensis biomass*

Biomass reusability was assessed to evaluate the environmental and economic facets. To determine the reusability of the biomass, an initial experiment was done to identify whether the alkaline (pH 10) or acid (pH 4) aqueous solute was more effective in desorbing/detaching the MNZ molecules from the used biomass. The findings from Fig. 6 revealed that the rate of MNZ removal for the biomass regenerated by the alkaline solution was higher. In Fig. 6 the MNZ removal rate is observed to drop from 60% in the first cycle to 54% in the fourth cycle. Hence, it can be deduced that this alga can remove the MNZ successfully to a maximum of four times after usage. The reduced removal may be caused by the active adsorption sites getting blocked, and the strong/chemical interactions present in nature, which induced changes in the surface heterogeneity (Bonyadi et al. 2021).

S. platensis, a blue-green, photosynthetic alga, has been found to have a variety of applications as a biosorbent. The BBD model was used to study the removal optimization of MNZ by *S. platensis*. From the findings it was observed that 88.15% of MNZ was removed from the reaction mixture by *S. platensis*, in the following settings: contact time of 38.05 min, MNZ level of 35 mg/L, pH of 7.71 and a biomass dose of 0.3 g/L. The quadratic model revealed that the chief variable affecting the MNZ removal rate was the MNZ concentration. The MNZ removal rate was thus seen to follow the pseudo-second-order model and Freundlich model. The fact that the MNZ biosorption process was spontaneous, exothermic and physical was evident from the thermodynamic data. Hence, the conclusion drawn was that the use of *S. platensis* was a cost-effective and successful way for the removal of MNZ from aqueous solutions. The results of this work ensure that for the removal of MNZ from aqueous solutions *S. platensis* can be successfully employed as a cheap, available and efficient biosorbent.

Acknowledgements Not applicable.

Authors' contributions All authors contributed to the study conception and discussions. ZE performed material preparation, data collection and analysis. BB studied materials characterization and tests. MS presented experiments and discussion. HA analyzed the results. TAM wrote and edited. ZB conceived and designed the experiments. All authors read and approved the final version of this manuscript.

Funding The authors extend their appreciation to Mashhad University of Medical Science for the financial support provided for the MSC dissertation, under Grant Number 991138.

Data availability All necessary data are included in the document.

Declarations

Conflict of interest The authors declare that they have no confict of interests.

Ethical approval This article does not contain any studies with human participants or animals performed by any of the authors.

References

Adel M, Ahmed MA, Mohamed AA (2021) Effective removal of indigo carmine dye from wastewaters by adsorption onto mesoporous magnesium ferrite nanoparticles. Environ Nanotechnol Monit Manage 16:100550

Ahmad MA, Puad NAA, Bello OS (2014) Kinetic, equilibrium and thermodynamic studies of synthetic dye removal using pomegranate peel activated carbon prepared by microwave-induced KOH activation. Water Resour Ind 6:18–35

Aliasghar Navaei M, Alidadid H, Dankoob M, Bonyadi Z, Dehghan A, Hosseini A (2019) Biosorption of reactive red 120 dye from aqueous solution using *Saccharomyces cerevisiae*: RSM analysis, isotherms, and kinetic studies. Desalin Water Treat 171:418–427

Bazzazzadeh R, Soudi M, Valinassab T, Moradlou O (2020) Kinetics and equilibrium studies on biosorption of hexavalent chromium from leather tanning wastewater by *Sargassum tenerrimum* from Chabahar-Bay Iran. Algal Res 48:101896

Bonyadi Z, Noghani F, Dehghan A, van der Hoek JP, Giannakoudakis DA, Ghadiri SK, Anastopoulos I, Sarkhosh M, Colmenares JC, Shams M (2021) Biomass-derived porous aminated graphitic nanosheets for removal of the pharmaceutical metronidazole: optimization of physicochemical features and exploration of process mechanisms. Colloids Surf A Physicochem Eng Asp 611:125791

Bonyadi Z, Nasoudari E, Ameri M, Ghavami V, Shams M, Sillanpää M (2022) Biosorption of malachite green dye over Spirulina platensis mass: process modeling, factors optimization, kinetic, and isotherm studies. Appl Water Sci 12(7):1–11

Brito LR, Ganiyu SO, dos Santos EV, Oturan MA, Martínez-Huitle CA (2021) Removal of antibiotic rifampicin from aqueous media by advanced electrochemical oxidation: role of electrode materials, electrolytes and real water matrices. Electrochim Acta 396:139254

Danish M, Ahmad T, Majeed S, Ahmad M, Ziyang L, Pin Z, Iqubal SS (2018) Use of banana trunk waste as activated carbon in scavenging methylene blue dye: kinetic, thermodynamic, and isotherm studies. Bioresour Technol Rep 3:127–137

Dotto G, Lima E, Pinto L (2012) Biosorption of food dyes onto Spirulina platensis nanoparticles: equilibrium isotherm and thermodynamic analysis. Bioresour Technol 103(1):123–130

Farzadkia M, Bazrafshan E, Esrafili A, Yang J-K, Shirzad-Siboni M (2015) Photocatalytic degradation of metronidazole with illuminated TiO_2 nanoparticles. J Environ Health Sci Eng 13(1):1–8

Gilca AF, Teodosiu C, Fiore S, Musteret CP (2020) Emerging disinfection byproducts: a review on their occurrence and control in drinking water treatment processes. Chemosphere 259:127476

Gondi R, Kavitha S, Kannah RY, Karthikeyan OP, Kumar G, Tyagi VK, Banu JR (2022) Algal-based system for removal of emerging pollutants from wastewater: a review. Bioresour Technol 344:126245

Jayakumar V, Govindaradjane S, Rajamohan N, Rajasimman M (2021) Biosorption potential of brown algae, Sargassum polycystum, for the removal of toxic metals, cadmium and zinc. Environ Sci Pollut Res 29(28):41909–41922

Jiang Q, Ngo HH, Nghiem LD, Hai FI, Price WE, Zhang J, Liang S, Deng L, Guo W (2018) Effect of hydraulic retention time on the performance of a hybrid moving bed biofilm reactor-membrane bioreactor system for micropollutants removal from municipal wastewater. Bioresour Technol 247:1228–1232

Kariim I, Abdulkareem A, Abubakre O (2020) Development and characterization of MWCNTs from activated carbon as adsorbent for metronidazole and levofloxacin sorption from pharmaceutical wastewater: kinetics, isotherms and thermodynamic studies. Scientific African 7:e00242

Kiki C, Rashid A, Zhang Y, Li X, Chen T-Y, Adéoye ABE, Peter PO, Sun Q (2021) Microalgal mediated antibiotic co-metabolism: Kinetics, transformation products and pathways. Chemosphere 292:133438

Kousha M, Farhadian O, Dorafshan S, Soofiani NM, Bhatnagar A (2013) Optimization of malachite green biosorption by green microalgae—Scenedesmus quadricauda and *Chlorella vulgaris*: application of response surface methodology. J Taiwan Inst Chem Eng 44(2):291–294

Liliana C, Inga Z, Ludmila R, Tatiana C, Ana P, Andrei A, Svetlana D, Larisa G, Decebal I (2021) Biomass of Arthrospira platensis enriched with lithium by bioaccumulation and biosorption process. Food Biosci 41:100950

Malakootian M, Olama N, Nasiri A (2019) Photocatalytic degradation of metronidazole from aquatic solution by TiO_2 doped Fe^{3+} nanophotocatalyst. Int J Envi Scie Technol 16(8):4275–4284

Mazloomi S, Bonyadi Z, Haghighat A, Nourmoradi H, Soori MM, Eslami F (2021) Removal of methylene blue by Saccharomyces cerevisiae: process modelling and optimization. Desalin Water Treat 236:318–325

Nasoudari E, Ameri M, Shams M, Ghavami V, Bonyadi Z (2021) The biosorption of Alizarin Red S by Spirulina platensis; process modelling, optimisation, kinetic and isotherm studies. Int J Environ Anal Chem 1–15. https://doi.org/10.1080/03067319.2020.1862814

Nasseh N, Barikbin B, Taghavi L, Nasseri MA (2019) Adsorption of metronidazole antibiotic using a new magnetic nanocomposite from simulated wastewater (isotherm, kinetic and thermodynamic studies). Compos Part B Eng 159:146–156

Nath J, Ray L (2015) Biosorption of Malachite green from aqueous solution by dry cells of *Bacillus cereus* M116 (MTCC 5521). J Environ Chem Eng 3(1):386–394

Pirsaheb M, Khodadadi T, Bonyadi Z, Sharafi K, Khosravi T (2013) Evaluation of pesticide residues 2, 4-D, Atrazine and Alachlor concentration in drinking water well of Mahidasht district-Kermanshah, Iran, 2010–2011. World App Sci J 23(11):1530–1537

Polianciuc SI, Gurzău AE, Kiss B, Ştefan MG, Loghin F (2020) Antibiotics in the environment: causes and consequences. Med Pharm Rep 93(3):231

Ramavandi B, Najafpoor AA, Alidadi H, Bonyadi Z (2019) Alizarin red-S removal from aqueous solutions using *Saccharomyces cerevisiae*: kinetic and equilibrium study. Desalin Water Treat 144:286–291

Sadeghi A, Ehrampoush MH, Ghaneian MT, Najafpoor AA, Fallahzadeh H, Bonyadi Z (2019) The effect of diazinon on the removal of carmoisine by *Saccharomyces cerevisiae*. Desalin Water Treat 137:273–278

Tang X, Huang Y, He Q, Wang Y, Zheng H, Hu Y (2021) Adsorption of tetracycline antibiotics by nitrilotriacetic acid modified magnetic chitosan-based microspheres from aqueous solutions. Environ Technol Innov 24:101895

Wan S, Hua Z, Sun L, Bai X, Liang L (2016) Biosorption of nitroimidazole antibiotics onto chemically modified porous biochar prepared by experimental design: kinetics, thermodynamics, and equilibrium analysis. Process Safety Environ Protec 104:422–435

Wang H, Shi W, Ma D, Shang Y, Wang Y, Gao B (2020) Formation of DBPs during chlorination of antibiotics and control with permanganate/bisulfite pretreatment. Chem Eng J 392:123701

Zambrano J, García-Encina PA, Hernández F, Botero-Coy AM, Jiménez JJ, Irusta-Mata R (2021) Removal of a mixture of veterinary medicinal products by adsorption onto a *Scenedesmus almeriensis* microalgae-bacteria consortium. J Water Proc Eng 43:102226